



HAL
open science

Quasi-Elastic Light Scattering Study of Highly Swollen Lamellar and “Sponge” Phases

Éric Freyssingeas, Didier Roux, Frédéric Nallet

► **To cite this version:**

Éric Freyssingeas, Didier Roux, Frédéric Nallet. Quasi-Elastic Light Scattering Study of Highly Swollen Lamellar and “Sponge” Phases. *Journal de Physique II*, 1997, 7 (6), pp.913-929. 10.1051/jp2:1997162 . jpa-00248486

HAL Id: jpa-00248486

<https://hal.science/jpa-00248486>

Submitted on 4 Feb 2008

HAL is a multi-disciplinary open access archive for the deposit and dissemination of scientific research documents, whether they are published or not. The documents may come from teaching and research institutions in France or abroad, or from public or private research centers.

L'archive ouverte pluridisciplinaire **HAL**, est destinée au dépôt et à la diffusion de documents scientifiques de niveau recherche, publiés ou non, émanant des établissements d'enseignement et de recherche français ou étrangers, des laboratoires publics ou privés.

Quasi-Elastic Light Scattering Study of Highly Swollen Lamellar and “Sponge” Phases

Éric Freyssingeas (*), Didier Roux and Frédéric Nallet (**)

Centre de recherche Paul-Pascal, CNRS, avenue du Docteur-Schweitzer, 33600 Pessac, France

(Received 19 November 1996, received in final form 18 February 1997, accepted 20 February 1997)

PACS.82.70.-y – Disperse systems

PACS.68.10.-m – Fluid surfaces and fluid-fluid interfaces

PACS.05.40.+j – Fluctuation phenomena, random processes, and Brownian motion

Abstract. — We investigate experimentally, using quasi-elastic light scattering the dynamical properties of highly swollen lamellar and “sponge” phases. In our system the structural sizes — smectic period for lamellar phases or characteristic cell size for “sponge” phases — may be changed continuously by adding solvent up to scales of the order of optical wavelengths, *i.e.* several thousand Å. We observe the usual hydrodynamic behaviour, with monoexponential relaxation in time and q^2 scaling in reciprocal space when working with moderately dilute systems. At higher dilutions, the behaviour is no longer hydrodynamic: a q^3 universal scaling is observed for both lamellar and “sponge” samples, with stretched-exponential relaxation in time and universal exponents for *unoriented* lamellar or “sponge” samples. The undulation mode is identified in our data on oriented lamellar phases, both in its hydrodynamic limit and beyond, which leads to a measurement of the bilayer bending modulus κ . A tentative interpretation is given for our data on “sponge” phases, also leading to an estimate for κ .

Résumé. — Nous étudions expérimentalement, par diffusion quasi-élastique de la lumière, les propriétés dynamiques de phases lamellaires et “éponge” très diluées. Les dimensions structurales — période smectique en phase lamellaire, taille caractéristique de la cellule en phase “éponge” — peuvent être accrues de façon continue, par adjonction de solvant, jusqu’à atteindre des échelles de plusieurs milliers d’angströms, c’est-à-dire comparables à la longueur d’onde de la lumière. Avec des échantillons de dilution moyenne nous observons le comportement hydrodynamique habituel : relaxation temporelle mono-exponentielle et loi de puissance en q^2 dans l’espace réciproque. Aux dilutions plus élevées, le comportement n’est plus hydrodynamique : une loi de puissance en q^3 est observée en phase lamellaire comme en phase “éponge” ; la relaxation temporelle suit une loi en exponentielle étirée, avec un exposant universel pour les phases lamellaires *non orientées* et les phases “éponge”. Le mode d’ondulation est identifié, dans sa limite hydrodynamique et au-delà, à partir de nos données sur les phases lamellaires orientées ce qui donne lieu à une mesure du module κ d’élasticité de courbure de la bicouche. Nous proposons une interprétation de nos données en phase “éponge” conduisant également à une estimation de κ .

(*) *Present address:* Fysikalisk Kemi 1, Kemicentrum, Box 124, 221 00 Lund, Sweden.

(**) Author for correspondence (e-mail: nallet@crpp.u-bordeaux.fr) also at: Université Bordeaux-I.

1. Introduction

Lamellar and “sponge” phases are rather common structures encountered in many multicomponent surfactant/solvent systems. In both phases the structural units are surfactant-based fluid *bilayers*. In the lamellar phase, bilayers with infinite lateral extension are periodically stacked along one direction, which gives to the system the symmetry of a smectic A liquid crystal [1]. The “sponge” phase, on the other hand, is an isotropic liquid characterized by the presence of two distinct, continuous solvent volumes separated by a multiply-connected surfactant bilayer [2–4].

The “sponge” as well as the lamellar structures define length scales that depend on concentration: the smectic period d , for lamellar phases or the size ξ of the random network built by the bilayer, for “sponge” phases. In certain systems, the surfactant concentration may be varied in an extremely wide range to yield lamellar or “sponge” length scales ranging from typically 5 nm at high concentrations to more than 1 μm in the very dilute limit [5–8]. These systems are then perfectly suited for studying such bilayer properties as *flexibility*, characterized by the elastic bending modulus κ [9] and *interactions*, since the idealization of a structureless membrane with no reference to its detailed molecular content becomes increasingly better with higher dilutions.

Among the various experimental techniques that have been proposed to study lamellar and “sponge” systems [10], dynamic light scattering has been used quite extensively [11–17]. This technique probes the dynamics of equilibrium concentration fluctuations at typical spatial and time scales, respectively, 0.3 – 3 μm and 10^{-6} –1 s. For moderately dilute lamellar or “sponge” phases, concentration fluctuations at such scales arise from the coupled motions of quite a large number of bilayers. Hydrodynamic theories are relevant to describe such motions [18–21] and have been used rather successfully to extract from the experimental light scattering spectra a whole wealth of information about elastic or thermodynamic properties of lyotropic phases [12, 13, 17]. In the very dilute limit, however, the characteristic structural lengths of either lamellar or “sponge” phases become so large that the motions probed by dynamic light scattering are no longer *collective*, in the sense that concentration fluctuations now arise from the displacement with respect to solvent of *isolated* bilayers. A somewhat similar situation obtains in the study of concentration fluctuations in other, classical systems with large structural lengths, namely multi-component mixtures close to a critical point [22], or (usually semi-dilute) solutions of very long polymers [23]. From the large amount of both experimental and theoretical work devoted to these last systems, a coherent picture of their dynamical properties has been gained. In particular, universal behaviours for the relaxation frequency as a function of wave vector, both properly scaled, are predicted and observed in the appropriate time-dependent, equilibrium correlation functions [24, 25].

It is the aim of the present paper to report about the experimental study, using dynamic light scattering techniques of very dilute lamellar and “sponge” phases. In Part 2, we briefly describe our systems and give results obtained with moderately dilute *oriented* lamellar phases, recalling the classical hydrodynamic interpretation [12, 19]. Part 3 gives our results with oriented lamellar phases of arbitrary dilution, in a study where the light scattering wave vector is *parallel* to the average bilayer plane; we suggest that the light scattering signal arises from the undulation mode of the lamellar phase. From the universal form of the correlation function associated to this mode, we deduce a measurement of the bilayer bending modulus κ . Results with dilute “sponge” phases are found in Part 4: non-exponential relaxations are observed, described as *stretched exponentials* with a quasi-universal dispersion relation, in reduced units, and a constant stretching exponent α at high dilution. Part 5 is concerned with the dynamic properties of *unoriented* lamellar phases — considered in the very dilute limit to be similar to

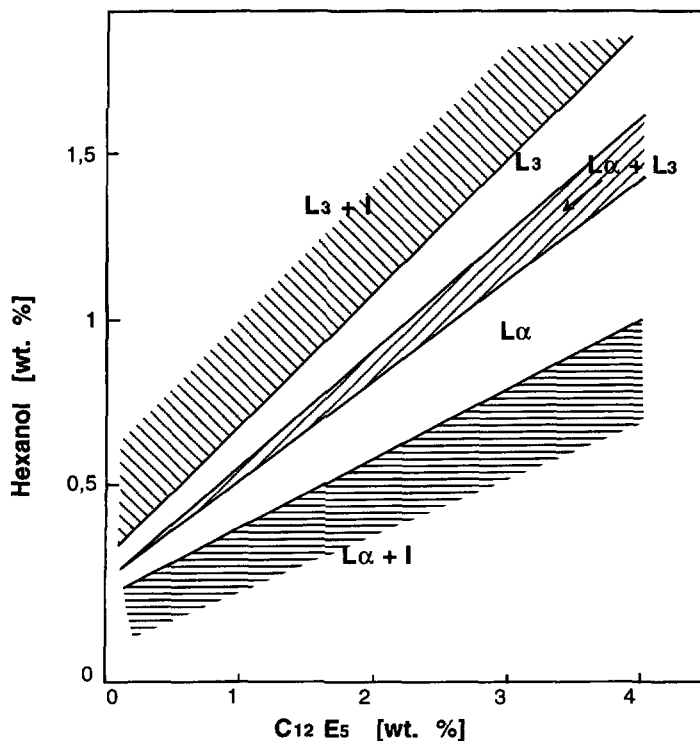


Fig. 1. — Dilute part of the phase diagram at room temperature for the $C_{12}E_5$ -1-hexanol-water system, with two one-phase domains (L_α , lamellar phase and L_3 , "sponge" phase) and two-phase equilibria (I, isotropic phases). Compositions are expressed in mass fractions.

"sponge" phases at the light scattering scale —, as well as with a discussion of our results. Using a recent theoretical investigation [26], it is argued that one may again extract an estimate for the bilayer bending modulus κ for both the "sponge" and the disoriented lamellar phases.

2. Phase Diagram and General Information

Most of the systems we are experimentally dealing with in this work are prepared with a non-ionic surfactant (n-dodecyl penta-ethyleneglycol monoether), referred to for short as $C_{12}E_5$, 1-hexanol and water. The first account of the phase diagram of this three-component solution may be found in reference [27]. Both lamellar and "sponge" phases are found at or close to room temperature in an extended range of concentrations, see Figure 1.

Samples are prepared along dilution lines by mixing various amounts of a concentrated, initial sample with solvent. Along the first dilution line, appropriate for studies on lamellar phases, the composition of the starting sample is: surfactant mass fraction $x_S \approx 0.55$, alcohol mass fraction $x_A \approx 0.15$. Working with "sponge" phases, the starting sample contains a higher amount of alcohol with composition: $x_S \approx 0.25$, $x_A \approx 0.11$. The solvent for both dilution lines is an aqueous solution of 1-hexanol with $x_A \approx 0.003$.

All samples on the first dilution line are lamellar phases at temperature $T = 24^\circ C$, at least up to a surfactant concentration as low as $x_S \approx 0.5\%$, as evidenced by the characteristic

smectic defects observed with a polarizing microscope and by their X-ray (or light) scattering spectra [28]. The smectic period reaches $d = 390$ nm for the most dilute sample. If one views the structure of the lamellar phase as $C_{12}E_5$ -alcohol bilayers of thickness δ separated by water, one expects a simple "swelling law" — relation between the smectic period d and the bilayer volume fraction ϕ — namely $d = \delta/\phi$ for *plane* bilayers. This relation is indeed obeyed with the most concentrated lamellar samples, yielding $\delta \approx 2.9$ nm. With more dilute samples the usual departure with a logarithmic correction is observed, attributed to the excess area stored in the increasingly crumpled bilayers, owing to undulation fluctuations [29–32]. This leads to a rough estimate for the bilayer bending modulus: $\kappa \approx 0.9k_B T$ [33].

Along the second dilution line, one has to adjust the temperature to remain in the isotropic, presumably "sponge" phase, found just above the lamellar phase [33]. The temperature varies between $T = 28.5$ °C for the most concentrated sample to $T = 24$ °C for the most dilute one, at $x_S \approx 0.2\%$. The "sponge" nature of the phase is revealed, apart from its close proximity to the lamellar phase in the phase diagram, by the characteristic *shape* of the X-ray or (static) light scattering spectra [3, 4, 34, 35]: hump at a wave vector q_0 that scales linearly with the bilayer volume fraction ϕ , q^{-2} decrease of the scattered intensity at large angles ($q > q_0$) and divergence of the intensity scattered at zero angle as ϕ^{-1} with a logarithmic correction. From the location of the hump in the scattering spectra it is possible to estimate the "size" of our most dilute sample to be: $\xi \approx 1.4$ μm .

The dynamic light scattering experiment is performed using a Coherent IK-90 ionized Krypton laser light source, operated at wavelength $\lambda = 647.1$ nm and linearly polarized vertically. Samples are held in glass cells immersed in a temperature-regulated, index matching liquid at the centre of a cylindrical cuvette with diameter 85 mm. The cells are cylindrical with diameter *ca.* 10 mm for "sponge" (or *disoriented* lamellar phases) and rectangular with cross-section 2×0.2 mm² for *oriented* lamellar samples. In this last case a special sample-holder is used: the angle ψ between the normal \mathbf{n} to the rectangular capillary and the scattering plane may be set equal to either 0 or 20 degrees; a goniometer determines the angle θ between the projection onto the scattering plane of the normal \mathbf{n} and the incident beam. The scattered light is collected with a photon-counting PMT (Hamamatsu), for scattering angles $\varphi = 20$ –160 degrees. A polarizer is used to analyze its polarization state. The photocurrent is processed with a 72-channel Brookhaven Instruments digital correlator that may be operated in a multiple-sample-time mode.

Once inside sealed capillaries, the lamellar samples are heated to the temperature of the lamellar/"sponge" transition and slowly (*ca.* -0.2 °C/min) cooled down. This usually yields oriented samples, with smectic layers parallel to the broad sides of the glass capillary in most of the volume, as checked by observations with a polarizing microscope: the samples appear black between crossed polarizers, with thin oily streaks close to the lateral boundaries of the capillary and a few edge-dislocation lines running parallel to the capillary axis, evidencing an almost perfect *homeotropic* alignment. "Sponge" samples, on the other hand, are quite sensitive to small external disturbances like gentle stirring or small temperature jumps. Flow birefringence is for instance induced by stirring motions; with the most dilute samples, it takes perhaps *hours* to relax. The "sponge" samples are thus allowed ample time to equilibrate on the light scattering set-up before doing the measurements. Reproducibility of their *static* light scattering spectra is used as a criterion for thermodynamic equilibrium.

The primary output of a dynamic light scattering experiment with homodyne detection is the time autocorrelation function of the scattered light intensity $\langle I(0)I(t) \rangle$. Assuming as usual Gaussian statistics for the fluctuations of the scattered field, we analyze the time behaviour

of the reduced correlation function $g_2(t) \equiv \langle I(0)I(t) \rangle / \langle I \rangle^2 - 1$ as the *square* of simple test functions:

$$\begin{aligned} \text{single exponential:} & \quad \exp(-\Omega t) \\ \text{stretched exponential:} & \quad \exp[-(\Omega t)^\alpha] \\ \text{cumulant expansion:} & \quad \exp[-(\Omega t + \beta_2 t^2 / 2)] \end{aligned}$$

where the parameter Ω describes in each of these test functions the characteristic relaxation frequency of the light scattering signal. The single exponential form is expected to hold when one mode only contributes to the signal, as should be the case with a perfectly oriented lamellar phase for instance [12, 19]; the other two functional forms are used only as convenient representations for different kinds of multiple-mode superpositions. In our experiment, we record the frequency parameter Ω (and, when appropriate, the stretching exponent α) as a function of the scattering angle φ , which sets the magnitude q of the scattering wave vector \mathbf{q} , with the polarizer set usually either parallel — VV configuration — or perpendicular — VH conf. — to the incident polarization, and varying (with oriented lamellar phases) the angle θ . When this last angle is scanned in the range $\varphi/2 - \varphi/2 + \pi/2$, the projection q_z of the scattering wave vector \mathbf{q} onto the optical axis increases from 0 to its maximum value $q \cos \psi$.

Three moderately dilute, oriented lamellar samples have been first studied with dynamic light scattering. The bilayer volume fractions are, respectively, $\phi = 40, 20$ and 8% . The corresponding smectic periods, as measured by X-ray scattering or interpolating the “swelling law” in the gap where Bragg peaks are no longer seen with X-ray, and not yet in the light scattering range are, respectively: $d = 7.4$ nm, $d \approx 15.5$ nm and $d \approx 44$ nm. There is a strong, VV signal for all three samples for all values of the scattering angle φ as long as the wave vector \mathbf{q} is close enough to the sample optical axis \mathbf{n} , *i.e.* when q_z is large enough. When q_z goes to zero, there is no reliable VV signal any more; a rather weak VH signal may be recorded, for the last two samples, quite easily up to $q_z = 0$ at small scattering angles φ or in its vicinity only, for larger angles. The VV and VH signals have the same time dependence when they may be recorded at a given $\{q, q_z\}$ configuration; moreover, the same is true for any orientation of the analyzing polarizer. The functional form of the signal is usually very close to a single-exponential time decay, with a lesser adequacy of this test function as q_z decreases. Nevertheless, both single exponential and cumulant expansion give similar results for the characteristic frequency Ω , with a somewhat better fit with the second expression, as may be expected. We therefore always used the cumulant expansion in our analysis.

The results with the $d \approx 15.5$ nm and $d \approx 44$ nm samples are displayed in Figure 2. The data, obtained in scanning the $\{q, q_z\}$ plane by varying both the scattering angle φ and the sample orientation angle θ [12] is displayed as a function of $q_\perp^2 \equiv q^2 - q_z^2$. Data following a given branch of the “candelabrum” is taken at a given *modulus* q of the scattering wave vector, which illustrates the strong anisotropy of the dynamic light scattering signal. Note also that the characteristic frequency varies extremely rapidly close to $q_z = 0$, near the tips of the “candelabrum”. This implies that any remaining orientational disorder in a lamellar sample is apt to cause a significant *broadening* of the signal spectral width in the vicinity of a nominally $q_z = 0$ configuration. As mentioned above, such a broadening is indeed experimentally observed near $q_z = 0$; it appears as a departure from the single-exponential time decay. Another important practical consequence is that the experiment always *underestimates* the “true” characteristic relaxation frequency at $q_z = 0$.

The data displayed in Figure 2 are well-described by the linear hydrodynamic theory of two-component smectic A liquid crystals [12, 19]. In this framework, the lowest frequency mode corresponds to layer displacement fluctuations — therefore associated in *general* (except

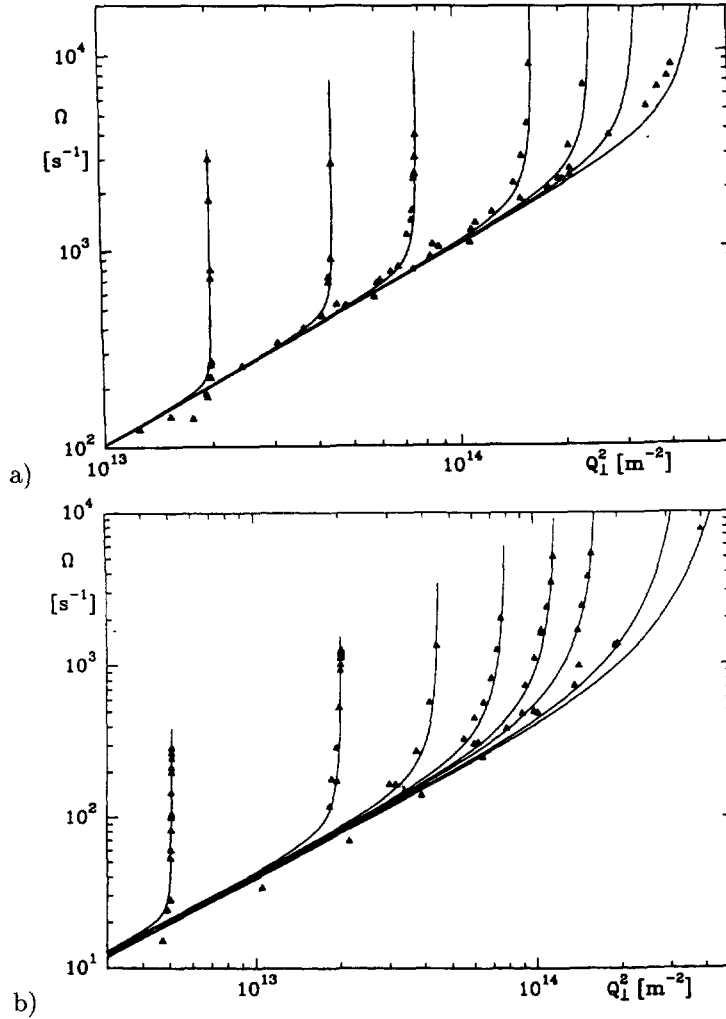


Fig. 2. — Relaxation frequencies Ω of the dynamic light scattering signal for oriented lamellar samples (Fig. 2a: $d \approx 15.5$ nm; Fig. 2b: $d \approx 44$ nm). Each “candelabrum” branch corresponds to a Q_{\perp} scan at a fixed value for the wave vector modulus Q . The lines come from a fit to the baroclinic mode dispersion relation, with the two elastic constants \bar{B} and K as adjustable parameters — see text.

for $q_z = 0$) with concentration fluctuations — coupled to solvent flow. This *baroclinic* mode, with dispersion relation [12, 36]:

$$\omega = \frac{\bar{B}q_z^2 + Kq_{\perp}^4}{\eta q^4 + q_z^2/\mu} q_{\perp}^2, \quad (1)$$

reduces to the usual *undulation* mode of one-component smectics A [37, 38] in the limit where the wave vector is parallel to the smectic layers, *i.e.* when $q_z = 0$.

In equation (1), \bar{B} is the smectic compression modulus at constant chemical potential [12, 19, 37], K the smectic splay modulus [37], η a viscosity and μ a dissipative parameter [19]. Taking these last two parameters equal, respectively, to the solvent (water) viscosity and to

the simplest available (Poiseuille flow) expression [19]:

$$\mu = \frac{d^2}{12\eta}, \quad (2)$$

(with d the smectic period and η the solvent viscosity), we fit equation (1) to our data with \bar{B} and K as adjustable parameters. While the compression modulus \bar{B} may be obtained for the three samples (increasing dilution, resp. $\bar{B} = 4.6 \times 10^3$ Pa, $\bar{B} = 5.0 \times 10^2$ Pa and $\bar{B} = 2.4 \times 10^1$ Pa), since it is associated with the common limiting *slope* of the dispersion relation (Eq. (1)), as q_{\perp} goes to zero,

$$\omega \sim \mu \bar{B} q_{\perp}^2, \quad (3)$$

the value for K is not reliable in the case of the most concentrated sample, owing to the lack of data in regions near $q_z = 0$ which determine the *height* of the “candelabrum” tips; with the last two samples we get, resp. $K \approx 1.5 \times 10^{-13}$ N and $K \approx 7 \times 10^{-14}$ N.

In the Helfrich model [39] of dilute lamellar phases, *flexible* bilayers characterized by a bending modulus κ undergo an effective, long-range repulsion because their undulation fluctuations are hindered by the presence of nearby bilayers in the lamellar stack. In the absence of any attractive interaction between bilayers [40], this mechanism leads to the following expression for the *smectic* elastic constants [39, 41, 42]:

$$\begin{cases} K = \kappa/d \\ \bar{B} = \frac{9\pi^2}{64} \frac{(k_B T)^2}{\kappa} \frac{d}{(d-\delta)^4} \end{cases} \quad (4)$$

which implies that the splay modulus K should scale inversely with the smectic spacing d , $K \sim d^{-1}$ and the compressibility modulus \bar{B} as d^{-3} . Obviously, our data does not permit a careful check of these scaling properties, even if a reasonable agreement is obtained. Assuming that our lamellar phase is indeed stabilized by Helfrich’s mechanism, we get using equation (4) two estimates for the value of the bilayer bending modulus κ :

$$\text{Splay modulus estimate:} \quad \kappa_K \approx 0.7 k_B T$$

$$\text{Compression modulus estimate:} \quad \kappa_{\bar{B}} \approx 3 k_B T.$$

Such a discrepancy between the two estimates seems to be frequently observed with dynamic light scattering on dilute lamellar systems [12, 13]; it might as well be due to experimental imperfections (residual orientational disorder, for instance) or to the crudeness of some of our theoretical assumptions (*e.g.* regarding the mobility parameter μ). Other experimental determinations of the elastic constants K and \bar{B} would be desirable to help settle that issue.

3. Dilute Lamellar Samples: $q_z = 0$

Three extremely dilute lamellar samples with bilayer volume fraction ϕ about 1% were prepared, adding solvent to the samples described previously. We checked, monitoring birefringence with a polarizing microscope that all along the dilution process the samples were always in the one-phase, lamellar region of the phase diagram. The most dilute samples have quite a small birefringence; they nevertheless display faint but characteristic oily streak defects. Moreover, as may be seen in Figure 3 a sharp, Bragg reflection is observed in light scattering — for powder samples. From the peak positions, the smectic spacings of the three dilute samples may be determined (increasing dilution): $d = 300$ nm, $d = 350$ nm and $d = 390$ nm.

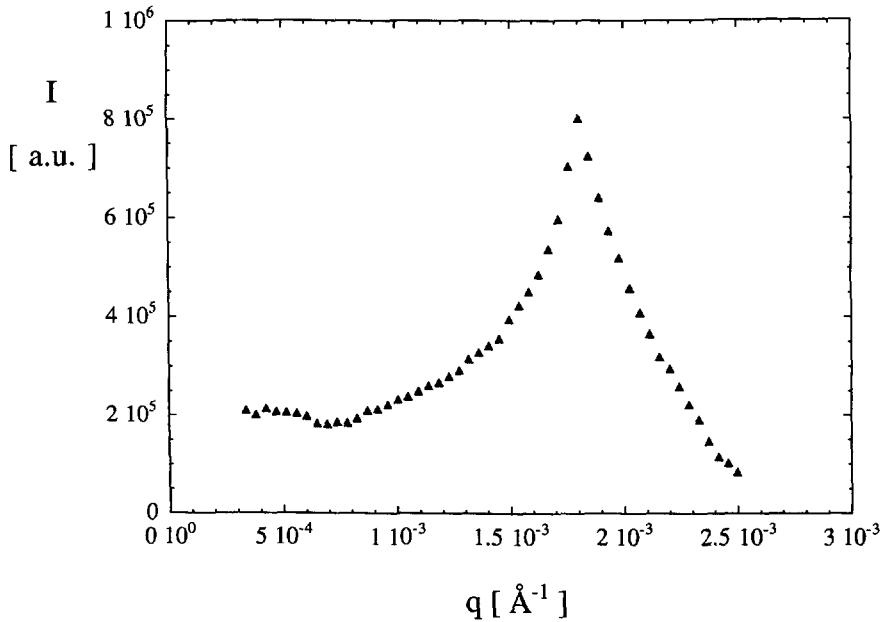


Fig. 3. — Static light scattering intensity for a non-oriented, very dilute lamellar sample. The bilayer volume fraction is: $\phi \approx 1.1\%$. From the sharp, Bragg reflection observed the smectic period is deduced to be: $d = 350$ nm.

Dynamic light scattering experiments have been performed with these three oriented samples, in both VV and VH configurations, keeping the scattering wave vector \mathbf{q} *parallel* to the smectic layers, *i.e.* with $q_z = 0$. Although both VV and VH signals are observed at intermediate scattering angles, there is no reliable VV signal at small angles (typically, φ smaller than about 20 degrees), nor any significant VH signal when the magnitude of the scattering wave vector reaches or exceeds the Bragg position q_0 .

The time decay of the light scattering signal has been fitted to either single-exponential or stretched-exponential test functions, with somewhat better results for the second choice. The stretching exponent α remains always close to 0.9, however. This illustrates that the departure from an exponential relaxation is weak. When both VV and VH signals are present at a given scattering angle, the former decays in time more rapidly than the latter. This is not related to a difference in stretching exponents — $\alpha_{VV} = \alpha_{VH} \approx 0.9$ —, but to a relaxation frequency larger for the VV signal than for VH. The relative difference increases with the scattering angle but remains limited: less than about 40% at worst.

We get from our analysis two dispersion relations, $\omega_{VV}(q, q_z = 0)$ and $\omega_{VH}(q, q_z = 0)$. Figure 4 displays the main features of both dispersion relations, for the sample with smectic period $d = 350$ nm. When it can be measured, ω_{VH} is roughly linear in q^2 . The same scaling is observed with ω_{VV} at small wave vectors but there is a cross-over, starting somewhat below q_0 , to a q^3 behaviour at larger scattering angles. As dilution increases the relaxation frequencies are inversely proportional to the smectic period in the q^2 regime but ω_{VV} stays constant in the q^3 regime. Using appropriate reduced variables, namely $\omega^* \equiv \frac{4\eta}{k_B T} \frac{\omega}{q^3}$ as reduced frequency (the prefactor $\frac{4\eta}{k_B T}$, with η the solvent viscosity is chosen for later convenience) and $q^* \equiv q/q_0$ as reduced wave vector, all the data, including the (VH) data at $q_z = 0$ for the last two moderately dilute samples described in Part 2 collapse onto a single universal curve, as shown in Figure 5.

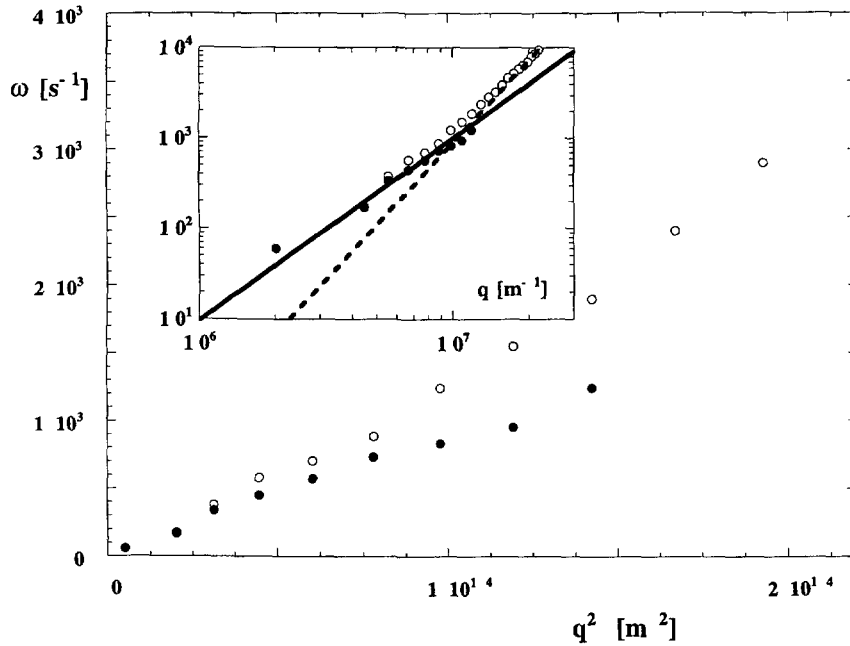


Fig. 4. — Polarized (o) and depolarized (•) relaxation frequencies at $q_z = 0$ as a function of the modulus q of the scattering wave vector. The inset in double logarithmic scale shows a cross-over from q^2 (thick line) to q^3 (broken line) scaling as the wave vector increases. The smectic period of the sample (same as in Fig. 3) is $d \equiv 2\pi/q_0 = 350$ nm. The Bragg position is $q_0 \approx 1.8 \times 10^7 \text{ m}^{-1}$

It is possible to interpret the universal behaviour observed in terms of the dynamics of the *undulation mode* of dilute lamellar phases. The coupled layer displacement–solvent flow fluctuations, occurring with a wave vector parallel to the average plane of the smectic layers may be described both in the hydrodynamic regime — the mode wavelength and relaxation time are much larger than any structural space and time scales in the system — and beyond, when the mode wave vector becomes comparable to the structural scale q_0 . In the latter case, the restoring force arises only from the splay elasticity of the smectic system (originating in bilayer bending elasticity for lamellar phases) whereas the solvent-mediated hydrodynamic interaction between neighbouring parts of a bilayer also comes into play in the former case [43–45]. The detailed analysis made in reference [44] leads to the following dispersion relation for the undulation mode:

$$\omega = \frac{\kappa \sinh(qd) + qd}{4\eta \cosh(qd) - 1} q^3, \tag{5}$$

where q is the modulus of the wave vector (recall that $q_z = 0$), d the smectic period, κ the bilayer bending modulus and η the solvent viscosity.

In the hydrodynamic limit ($qd \ll 1$) equation (5) reduces to equation (1) taken at $q_z = 0$ since $K = \kappa/d$. In the opposite limit ($qd \gg 1$) one gets:

$$\omega = \frac{\kappa}{4\eta} q^3. \tag{6}$$

Using the above-defined reduced variables ω^* and q^* , equation (5) may be recast into the

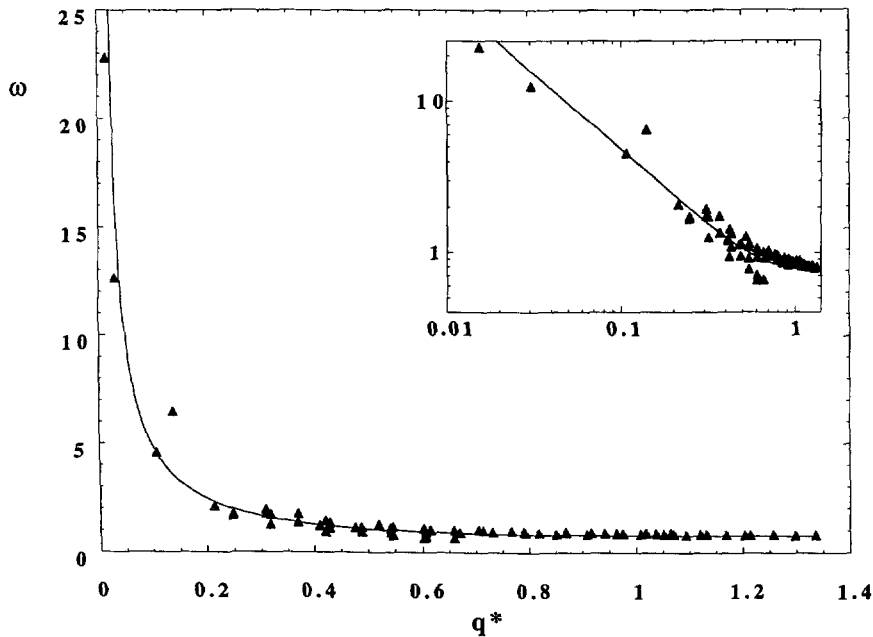


Fig. 5. — Reduced frequency ω^* as a function of the reduced wave vector q^* for all the VV or VH data taken at $q_z = 0$ on moderately or extremely dilute, oriented lamellar phases. The continuous curve is a one-parameter fit to the model discussed in the text, yielding a bilayer bending modulus $\kappa = 0.75k_B T$.

simple form $\omega^* = \mathcal{M}(q^*)$ with the Messenger function defined as:

$$\mathcal{M}(x) = \frac{\kappa}{k_B T} \frac{\sinh(2\pi x) + 2\pi x}{\cosh(2\pi x) - 1} \quad (7)$$

The continuous curve superimposed to the data shown in Figure 5 results from a fit to the Messenger function, with only one adjustable parameter, namely $\kappa/k_B T$. From the quite good agreement between experiment and model it seems adequate to conclude that our light scattering experiment on oriented lamellar phases either moderately or extremely dilute is sensitive to the undulation mode. The experiment leads then to an estimate of the $C_{12}E_5$ -hexanol bilayer bending modulus $\kappa = 0.75k_B T$. Since this value is very nearly identical to the splay modulus estimate κ_K obtained Part 2, we conclude that the bending modulus softening predicted to occur at long wavelengths owing to renormalization effects [46, 47] is not observable with the present experiment.

4. Dilute “Sponge” Phases

We performed our light scattering experiment on eight “sponge” samples ($C_{12}E_5$ -hexanol-water system), with bilayer volume fraction ranging from $\phi \approx 5.3\%$ for the most concentrated sample to $\phi \approx 0.4\%$ for the most dilute one. The “sponge” phase, though optically isotropic is built with *anisotropic* surfactant bilayers. Besides, anisotropic concentration fluctuations may in principle occur. Therefore, depolarized scattering is to be expected [48]. When observable — with the more dilute “sponge” samples — the depolarized signal is small, about 10^3 less

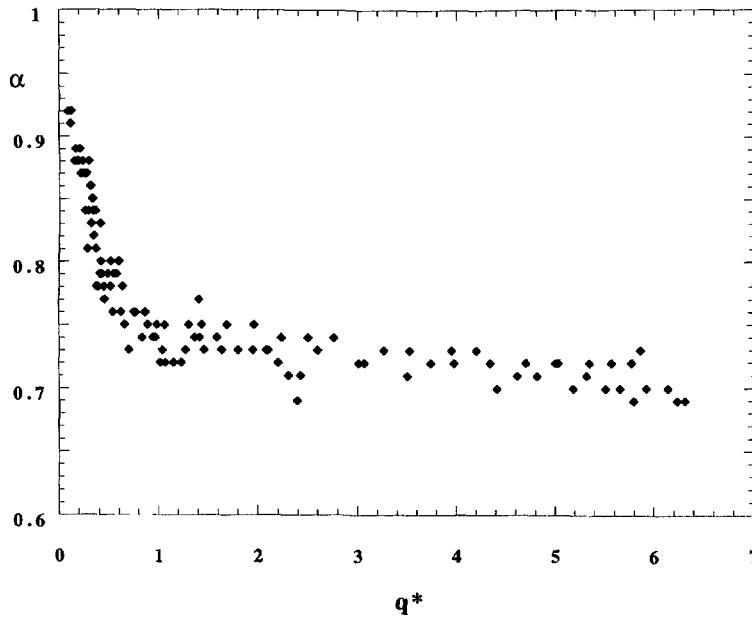


Fig. 6. — Stretching exponent α as a function of the reduced scattering wave vector q^* for all the $C_{12}E_5$ “sponge” samples.

intense than the VV one. The depolarized scattering was not systematically recorded: we have checked that there was no significant difference in time behaviour and dispersion properties between depolarized and VV signals.

The time decay of the (VV) light scattering signal is definitely not a single-exponential with our “sponge” samples. On the other hand, the stretched-exponential test function yields a very good fit to the data. The stretching exponent α decreases significantly from about 0.9 to about 0.7 as the scattering wave vector increases and as the samples become more dilute. As shown in Figure 6 — which summarizes our results for the eight “sponge” samples —, α follows a single, universal curve when plotted as a function of the reduced scattering wave vector $q^* \equiv q/q_0$. Here, q_0 is the measured or extrapolated location of the hump in *static* scattering spectra (see Part 2). The initial decrease in α at small q^* is followed by a regime, for $q^* \geq 1$, where the stretching exponent is constant or perhaps weakly decreasing.

The typical shape of the dispersion relation $\omega(q)$ is illustrated in Figure 7: the cross-over from a q^2 to a q^3 scaling, already observed with oriented lamellar phases (see Part 3) also obtains with “sponge” samples. As it appears in varying the bilayer concentration, the location in reciprocal space of the cross-over region as well as the slope of the ω vs. q^2 line are concentration-dependent. This is perhaps better seen in Figure 8, where the reduced relaxation frequency $\omega^* \equiv \frac{12\pi^2\eta}{k_B T} \frac{\omega}{q^3}$ — η is the *solvent* viscosity and the numerical prefactor $12\pi^2$ is somewhat arbitrarily chosen — is plotted as a function of the reduced wave vector q^* for the six most dilute “sponge” samples. The reduced frequency ω^* reaches a constant, asymptotic value — here about 1.8 with our choice for the numerical prefactor $12\pi^2$ — for large values of the scattering wave vector, $q^* \geq 2$. At contrast, in the lower q^* range, the reduced relaxation frequency does not seem to follow a single universal curve; besides, it varies non-monotonically, decreasing *below* the asymptotic value for q^* in the range 1/2–2.

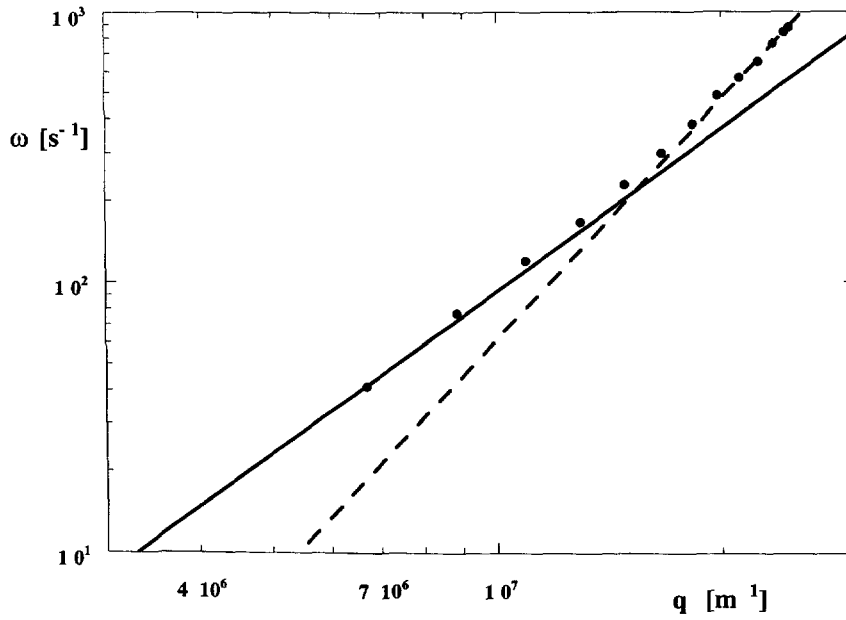


Fig. 7. — Relaxation frequency ω — extracted from the stretched-exponential analysis — as a function of the scattering wave vector q . The double logarithmic scale shows the cross-over from a q^2 (thick line) to a q^3 (broken line) scaling as the wave vector increases.

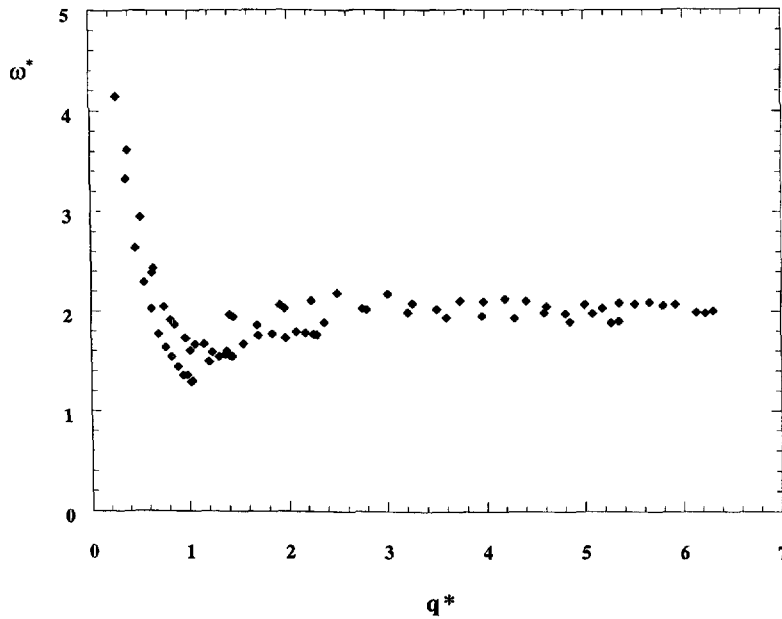


Fig. 8. — Reduced relaxation frequency ω^* as a function of the reduced scattering wave vector q^* , for all the $C_{12}E_5$ "sponge" samples.

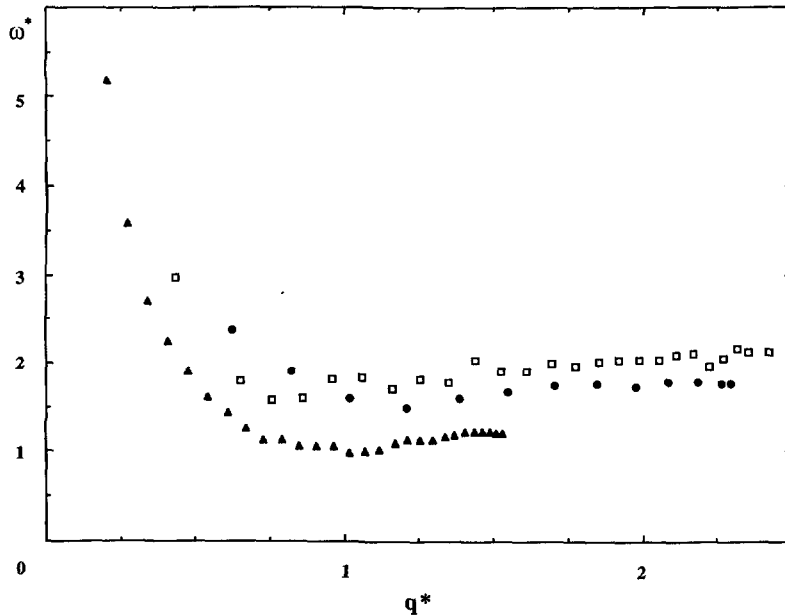


Fig. 9. — Reduced relaxation frequencies ω^* as a function of reduced scattering wave vectors q^* , for “sponge” samples belonging to three different families; triangles: SDS/octanol/brine; circles: $C_{12}E_5$ /hexanol/water; squares: SDS/water/pentanol/dodecane.

Most of the features observed with the dilute “sponge” phases in the $C_{12}E_5$ -hexanol-water solutions are in fact common to other “sponge” systems: we have indeed prepared such phases with either a direct, ionic surfactant bilayer swollen in brine (sodium dodecylsulphate or SDS, 1-octanol and 20 g/l sodium chloride water solution [49]) or a reverse bilayer swollen in oil (SDS/water/1-pentanol/dodecane [50]). Stretched-exponential instead of single-exponential relaxations are always found, with stretching exponents α close to those measured in the non-ionic system at similar values for the reduced wave vector q^* . Moreover, the reduced frequency ω^* — defined of course with the appropriate solvent viscosity — also reaches an asymptotic value at large q^* . This asymptotic frequency depends on the nature of the system, however: it is largest with the reverse, SDS system, intermediate with the non-ionic system and smallest with the direct, SDS system, see Figure 9. This dependence could arise from differences in the bilayer bending moduli κ for these three systems. Indeed, according to dynamic light scattering experiments on (oriented and more concentrated) *lamellar* phases built with the same bilayers one has: $\kappa \approx 4k_B T$ in the SDS/octanol/brine system [51], $\kappa \approx 3k_B T$ in the $C_{12}E_5$ /hexanol/water system (see Part 2) and $\kappa \approx 2k_B T$ in the SDS/water/pentanol/dodecane system [12], where all three values are given here from *compression modulus* estimates. Our results therefore suggest that the characteristic decay rate in “sponge” phases is a *decreasing* function of the bilayer bending modulus, at least in the asymptotic regime where $q\xi \gg 1$.

5. Final Results and Discussion

In order to illustrate from a dynamic point of view the structural identity at *local* scales between lamellar and “sponge” phases, we have studied by dynamic light scattering a *disoriented*

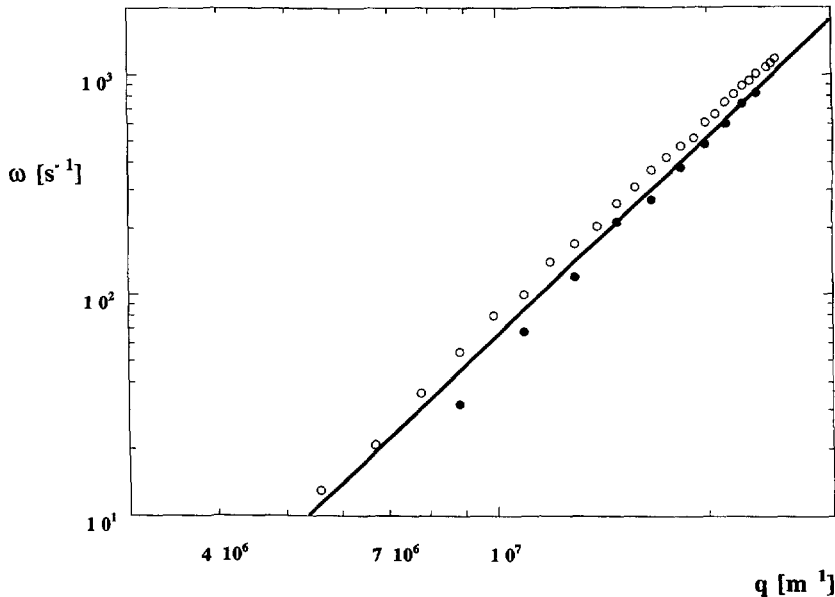


Fig. 10. — Relaxation frequencies as a function of the scattering wave vector q in double logarithmic scale for both “sponge” (○) and *disoriented* lamellar (●) $C_{12}E_5$ samples at about the same dilution. The straight line corresponds to a q^3 scaling.

lamellar sample. Disorientation is achieved by quenching the sample prepared in the high temperature, “sponge” state into the lamellar phase. The sample — here, our most dilute lamellar phase with smectic period $d = 390$ nm —, held in a 10 mm diameter cylindrical light scattering cell, is quickly immersed in freezing water for 10–20 s. This procedure usually leads to a nearly random orientation of quite small lamellar crystallites. Such a “powder” orientation remains stable for a few hours if care is taken not to shake nor stir the sample.

For scattering wave vectors q smaller than the Bragg position q_0 it was not possible to record any reproducible light scattering signal, perhaps because the (slow) intrinsic dynamics associated with membrane fluctuations was blurred by the coarsening of our “powder”. On the other hand, quite a nice and reproducible VV signal may be recorded at larger wave vectors when the spatial scales probed are about or less the smectic spacing. The time decay is then well-described by a stretched exponential test function, with the exponent $\alpha \approx 0.7$ not significantly depending on the q value. The q^3 scaling for the characteristic relaxation frequency previously observed is obeyed here too, Figure 10. Moreover, as also illustrated in Figure 10, the relaxation frequencies are very nearly the same for the disoriented lamellar and “sponge” samples at similar dilutions: as expected, the “sponge” and lamellar structures, locally identical, have locally closely related bilayer dynamics.

Recently, the dynamics of membrane — lamellar and “sponge” — phases has been theoretically investigated by Zilman and Granek [26] in the regime where a single membrane description is appropriate, *i.e.* for local enough spatial scales. It is argued in reference [26] that the dynamic structure factor is then mostly controlled by the undulation dynamics of (on the average) flat pieces of membrane with arbitrary, but fixed, orientations with respect to the wave vector direction. It results that, in contrast to the case where the wave vector lies *exactly* within the membrane plane (undulation dynamics leading to an *exponentially*—

Table I. — *Experimental* (ω_{exp}^*) *and theoretical* (ω_{th}^*) *asymptotic relaxation frequencies in reduced units for three different dilute “sponge” systems* (κ : bilayer bending modulus).

“Sponge” systems	$\kappa/k_{\text{B}}T$	ω_{th}^* (Eq. (10))	ω_{exp}^* (Fig. 9)
SDS–octanol (direct bilayers)	4	1.13	1.2
C ₁₂ E ₅ –hexanol (direct bilayers)	3	1.30	1.8
SDS–pentanol (inverted bilayers)	2	1.60	2.1

decaying signal; characteristic frequency *linearly increasing* with κ [43, 44]), the signal has an anomalous stretched exponential dependence with a relaxation rate *decreasing* with increasing bending stiffness. The experimentally relevant dynamic structure factor for both “sponge” and randomly oriented lamellar phases is predicted to be [26]:

$$S(q, t) \sim \exp \left[- (\Gamma_q t)^{2/3} \right], \quad (8)$$

with the relaxation rate Γ_q close to:

$$\Gamma_q \simeq 0.019 \left(\frac{k_{\text{B}}T}{\kappa} \right)^{1/2} \frac{k_{\text{B}}T}{\eta} q^3. \quad (9)$$

The functional form of equation (8), as well as the κ and q scalings in equation (9) in fact appear as special cases within the framework of the very general theoretical study by Frey and Nelson [52] of the dynamics of fluid or polymerized “membranes”. It is to be noted that they are also in excellent *quantitative* agreement with our data: the predicted stretching exponent, namely 2/3, is close to the experimentally observed one: $\alpha \approx 0.7$ for both “sponge” and disoriented lamellar phases; more remarkably, the numerical prefactor and bending rigidity scaling in equation (9) translate into the following form for the reduced relaxation frequency, defined Part 4:

$$\omega^* \simeq 2.25 \left(\frac{k_{\text{B}}T}{\kappa} \right)^{1/2}, \quad (10)$$

which describes rather nicely the data in Figure 9, as summarized in Table I.

6. Conclusion

As we have shown in the present work, quasi-elastic light scattering techniques are suitable to study the dynamics of bilayer fluctuations in highly swollen lamellar and “sponge” phases. Polarized as well as depolarized scattering experiments are probing the same dynamical characteristics of the bilayer bending distortions, with a much better practical efficiency for polarized scattering in the high dilution limit.

The undulation mode is identified in studying *oriented* lamellar samples of the C₁₂E₅–1-hexanol–water system with a scattering geometry such as to keep the scattering wave vector parallel to the bilayer plane. From moderate to extremely high dilutions, the dynamic structure

factor is well-described by single exponential test functions with characteristic relaxation frequencies in good agreement with Messenger's prediction [44]; this leads to a measurement of the bilayer bending modulus, namely $\kappa \approx 0.75k_{\text{B}}T$ with no hints of any renormalization-induced softening of κ .

Essentially identical dynamical properties are found for extremely dilute, randomly *disoriented* lamellar samples and "sponge" samples when the scattering wave vector q becomes larger than the reciprocal of the structural size d (smectic period) or ξ ("sponge" cell size). The dynamic structure factor is then described by stretched exponential test functions, with an universal stretching exponent α , found close to 0.7 in three different (direct or inverted) bilayer systems. The characteristic relaxation frequencies are independent of the structural size and scale with q^3 . In contrast to the behaviour expected for the undulation mode, these relaxation frequencies *decrease* with *increasing* the bilayer bending stiffness κ . These features are in reasonable quantitative agreement with the recent model by Zilman and Granek [26], which may allow a new and experimentally appealing way to measure the elastic modulus κ in very dilute bilayer phases.

Acknowledgments

We owe special gratitude to Reinhard Strey for investigating the C_{12}E_5 -hexanol system, in the spirit of looking for a highly dilute lamellar phase at room temperature. We are grateful to Anton Zilman and Rony Granek for fruitful discussions and for sharing with us reference [26] prior to publication. We thank Erwin Frey for bringing to our attention reference [52].

References

- [1] Ekwall P., *Advances in Liquid Crystals*, Vol. 1, G.M. Brown Ed. (Academic Press, New York) 1975, p. 1.
- [2] Cates M.E., Roux D., Andelman D., Milner S.T. and Safran S.A., *Europhys. Lett* **5** (1988) 733.
- [3] Porte G., Marignan J., Bassereau P. and May R., *J. Phys. France* **49** (1988) 511.
- [4] Gazeau D., Bellocq A.-M., Roux D. and Zemb Th., *Europhys. Lett.* **9** (1989) 477.
- [5] Larché F.C., Appell J., Porte G., Bassereau P. and Marignan J., *Phys. Rev. Lett.* **56** (1986) 1700.
- [6] Satoh N. and Tsujii K., *J. Phys. Chem.* **91** (1987) 6629.
- [7] Appell J., Bassereau P., Marignan J. and Porte G., *Colloid Polym. Sci.* **267** (1989) 600.
- [8] Inae T., Sasaki M. and Ikeda S., *J. Coll. Interface Sci.* **131** (1989) 601.
- [9] Helfrich W., *Z. Naturforsch.* **28c** (1973) 693.
- [10] See, *e.g.*, *Micelles, Membranes, Microemulsions and Monolayers*, W.M. Gelbart, A. Ben-Shaul and D. Roux, Eds. (Springer-Verlag, New York, 1994).
- [11] Chan W. and Pershan P.S., *Phys. Rev. Lett.* **39** (1977) 1368.
- [12] Nallet F., Roux D. and Prost J., *J. Phys. France* **50** (1989) 3147.
- [13] Bassereau P., Thesis of University of Montpellier-II (1990).
- [14] Mangalampalli S., Clark N.A. and Scott J.F., *Phys. Rev. Lett.* **67** (1991) 2303.
- [15] Fabre P., Quilliet C., Veyssié M., Nallet F., Roux D., Cabuil V. and Massart R., *Europhys. Lett.* **20** (1992) 229.
- [16] Zhang C.Y., Sprunt S. and Litster J.D., *Phys. Rev. E* **48** (1993) 2850.

- [17] Porte G., Delsanti M., Billard I., Skouri M., Appell J. and Marignan J., *J. Phys. II France* **1** (1991) 1101.
- [18] Martin P.C., Parodi O. and Pershan P.S., *Phys. Rev. A* **6** (1972) 2401.
- [19] Brochard F. and de Gennes P.-G., *Pramana Suppl.* N° 1 (1975) 1.
- [20] Milner S.T., Cates M.E. and Roux D., *J. Phys. France* **51** (1990) 2629.
- [21] Granek R. and Cates M.E., *Phys. Rev. A* **46** (1992) 3319.
- [22] Kawasaki K., *Ann. Phys. N.Y.* **61** (1970) 1; Ferrel R.A., *Phys. Rev. Lett.* **24** (1970) 169.
- [23] de Gennes P.-G., *Scaling Concepts in Polymer Physics* (Cornell University Press, Ithaca, 1979); Doi M. and Edwards S.M., *The Theory of Polymer Dynamics* (Clarendon, Oxford, 1986).
- [24] Swinney H.L. and Henry D.L., *Phys. Rev. A* **8** (1973) 2586; Sengers J.M.H.L., *Pure Appl. Chem.* **55** (1973) 437.
- [25] Adam M. and Delsanti M., *Macromolecules* **10** (1977) 1229; Richter D., Binder K., Ewen B. and Stühn B., *J. Phys. Chem.* **88** (1984) 6618.
- [26] Zilman A.G. and Granek R., *Phys. Rev. Lett.* **77** (1996) 4788.
- [27] Jonströmer M. and Strey R., *J. Phys. Chem.* **96** (1992) 5993.
- [28] Freyssingeas É., Thesis of University of Bordeaux-I (1994).
- [29] Helfrich W. and Servuss R.M., *Nuovo Cimento* **3** (1984) 137.
- [30] Strey R., Schomäcker, Roux D., Nallet F. and Olsson U., *J. Chem. Soc. Faraday Trans.* **86** (1990) 2253.
- [31] Roux D., Nallet F., Freyssingeas É., Porte G., Bassereau P., Skouri M. and Marignan J., *Europhys. Lett.* **17** (1992) 575.
- [32] Freyssingeas É., Roux D. and Nallet F., *J. Phys.: Condens. Matter* **8** (1996) 2801.
- [33] Freyssingeas É., Nallet F. and Roux D., *Langmuir* **12** (1996) 6028.
- [34] Roux D., Cates M.E., Olsson U., Ball R.C., Nallet F. and Bellocq A.-M., *Europhys. Lett.* **11** (1990) 229.
- [35] Roux D., Coulon C. and Cates M.E., *J. Phys. Chem.* **96** (1992) 4174.
- [36] Sigaud G., Garland C.W., Nguyen H.T., Roux D. and Milner S.T., *J. Phys. II France* **3** (1993) 1343.
- [37] de Gennes P.-G., *J. Phys. Colloq. France* **30** (1969) C-65.
- [38] Ribotta R., Salin R. and Durand G., *Phys. Rev. Lett.* **32** (1974) 6; Birecki H., Schaetzing R., Rondelez F. and Litster J.D., *Phys. Rev. Lett.* **36** (1976) 1376.
- [39] Helfrich W., *Z. Naturforsch.* **33a** (1978) 305.
- [40] Milner S.T. and Roux D., *J. Phys. I France* **2** (1992) 1741.
- [41] Roux D. and Safinya C.R., *J. Phys. France* **49** (1988) 307.
- [42] Lubensky T.C., Prost J. and Ramaswamy S., *J. Phys. France* **51** (1990) 70.
- [43] Brochard F. and Lennon J.F., *J. Phys.* **11** (1975) 1035.
- [44] Messenger R., Bassereau P. and Porte G., *J. Phys. France* **51** (1990) 1329.
- [45] Ramaswamy S., Prost J., Cai W. and Lubensky T.C., *Europhys. Lett.* **23** (1993) 271.
- [46] Helfrich W., *J. Phys. France* **46** (1985) 1263.
- [47] Peliti L. and Leibler S., *Phys. Rev. Lett.* **54** (1985) 1690.
- [48] Aragon S.R. and Pecora R., *J. Chem. Phys.* **66** (1977) 2506.
- [49] Hervé P., Roux D., Bellocq A.-M., Nallet F. and Gulik-Krzywicki T., *J. Phys. II France* **3** (1993) 1255.
- [50] Roux D. and Bellocq A.-M., *Physics of Amphiphiles: Micelles, Vesicles and Microemulsions*, V. Degiorgio and M. Corti, Eds. (North-Holland, Amsterdam) 1985, p. 842.
- [51] Hervé P., Bellocq A.-M., Roux D., Nallet F. and Gulik-Krzywicki T., *unpublished*.
- [52] Frey E. and Nelson D., *J. Phys. I France* **1** (1991) 1715.